

# The Analysis of Spaceborne SAR Interferometry Based on Strapdown Inertial Navigation Mechanism and Maximum Likelihood Method

Shuguang Lei\*, Liu Zhang, Wenpan Li

Guangzhou Civil Aviation College, Guangzhou, Guangdong 510403, China  
 leishuguang@caac.net

In this paper, a spaceborne SAR interferometry system operates on the strapdown inertial navigation mechanism, which is based on maximum likelihood phase estimation method. It has been shown using simulated data that phase estimation of cross-track multi-baseline synthetic aperture radar (SAR) interferometric data is most efficiently achieved through a maximum likelihood phase estimation method. With the help of strapdown inertial navigation mechanism and compared to simulated data, dealing with real data implies that several calibration steps be carried out to ensure that the data fits the model. It is well known that a nonlinear frequency-modulation (NLFM) chirp waveform can shape the signal's power spectral density and provide a radar matched filter output with lower sidelobes without loss of the signal-to-noise ratio. The strapdown inertial navigation mechanism can measure the apex angle and azimuth angle, the motion attitude of the carrier can be calculated by the three-axis displacement and revolution which are measured by this system. Compares the value of spaceborne SAR interferometry with the value which is measured by strapdown inertial navigation mechanism, the measurement accuracy will be improved by the analysis of strapdown inertial navigation mechanism and maximum likelihood phase estimation method.

## 1. Introduction

Synthetic aperture radar (SAR) is a form of radar which is used to create images of objects, such as landscapes – these images can be either two or three dimensional representations of the object. Cross-track synthetic aperture radar (SAR) interferometry (InSAR) typically uses two receiving antennas forming a single baseline (Magnard et al., 2016). The length of this baseline must be chosen as a tradeoff. Interferograms generated using short baselines are easy to unwrap but have high sensitivity to a constant phase noise level in this way. SAR uses the motion of the radar antenna over a targeted region to provide finer spatial resolution than is possible with conventional beam-scanning radars. SAR is typically mounted on a moving platform such as an aircraft or spacecraft, and has its origins in an advanced form of side-looking spaceborne radar (SLAR) (Yang et al., 2015). The data from shorter baselines help unwrap interferograms based on longer baselines, and the lower relative noise level from the longer baselines is maintained in the composite solution.

There are several InSAR data processing methods for measuring spatical trajectory, such as the maximum likelihood method, the coarse-fine phase unwrapping method, and least squares and weighted least squares methods. The maximum likelihood method calculates a most-likely phase from arrays of focused SAR data [single look complex (SLC) data] according to a model. This allows use of all the data and should, therefore, improve the noise level and reliability (Schmitt et al., 2015). The coarse-to-fine phase unwrapping method uses data from the shorter baselines to unwrap the interferogram based on the longest baseline. This method keeps the unwrapped phase information from the longest baseline, discarding information from the other baselines. Several other methods such as least squares or weighted least squares can also be used to calculate the unwrapped phase; they are compared in showing their advantages and shortcomings. Multi-baseline maximum likelihood phase estimation is extended to handle multi-aspect data in results from single and multi-pass, multi-baseline InSAR acquisitions with the PAMIR sensor are presented in this paper.

A single-pass multi-baseline tomography concept is demonstrated in] using millimeter wave experimental multi-frequency polarimetric high-resolution interferometric system (Yang et al., 2015).

Properties of spaceborne single-pass multi-baseline data is also investigated using simulated data. Phase estimation based on multi-baseline interferometric SAR data is investigated using actual or simulated spaceborne systems. The technical parameters of these spaceborne systems are shown in table 1, such as PAMIR, MEMPHIS and OrbiSAR.

Table 1: The technical parameters of spaceborne systems

Technical parameters	PAMIR	MEMPHIS	OrbiSAR
Bandwidth	880MHz	900MHz	900MHz
Typical velocity	75m/s	78m/s	75m/s
Altitude	300-800m	350-1000m	250-700m
Azimuth angle	22° - 35°	20° - 40°	22° - 30°
Theoretical resolution precision	0.15m	0.11m	0.11m

As shown in table 1, the MEMPHIS spaceborne system has the wider bandwidth, higher typical velocity and wider azimuth angle. Its issues such as dissimilar receiver properties leading to different antenna phase patterns, nonperfectly aligned phase centers, and inaccuracies in the motion compensation can decrease the phase estimation accuracy. On the other hand, these airborne single-pass systems use baselines order of magnitudes shorter than the critical baseline, atmospheric effects are similar for all receivers, and temporal decorrelation is not present as all baselines are acquired in a single pass.

This paper puts forward a spaceborne SAR interferometry system operates on the strapdown inertial navigation mechanism, which is based on maximum likelihood phase estimation method, and this main research within this paper is: do maximum likelihood phase estimation of real airborne single-pass data quickly and effectively, and with a lower noise level. With the help of strapdown inertial navigation mechanism and compared to simulated data, dealing with real data implies that several calibration steps be carried out to ensure that the data fits the model. Compares the value of spaceborne SAR interferometry with the value which is measured by strapdown inertial navigation mechanism, the measurement accuracy will be improved by the analysis of strapdown inertial navigation mechanism and maximum likelihood phase estimation method. In data processing method, more outliers were generated with this method, and the noise level was almost identical for both methods.

## 2. System measurement principle and its technical parameters

The strapdown inertial navigation system is a trend of inertial technology in recent years, and combined navigation system based on inertial technology is paid attention to and developed (Perez et al., 2010). Inertial navigation technology is completely independent of the measurement method, it does not depend on the external light, electromagnetic wave, sound, magnetic field and so on external information to measure the object angular motion and linear motion, so the working mode completely unaffected by the interference effects of the external environment.

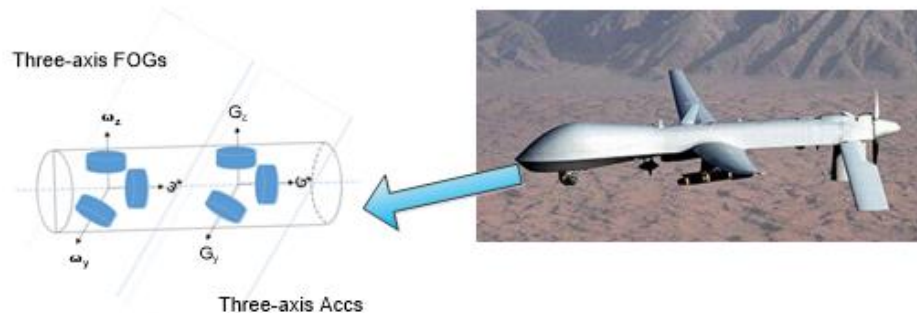


Figure 1: The measurement components of the strapdown inertial navigation system

## 2.1 System measurement principle

As shown in figure 1, the measurement system in this paper consists of three-axis pairwise orthogonal FOGs and three-axis pairwise orthogonal accelerometers, the FOG measures the components of earth self-rotation angle velocity, the accelerometer measures the components of earth gravity acceleration, the motion attitude of the carrier can be calculated by the three-axis displacement and revolution which are measured by the system.

The strapdown inertial navigation system consists of several coordinate systems, which are inertial coordinate system, carrier coordinate system, geography coordinate system and navigation coordinate system. Table 2 shows the definitions of these coordinate systems.

Table 2: Definitions of coordinate systems

Coordinate systems	Definitions
Inertial	Call I system for short. The coordinate system is also called the earth fixed coordinate system.
Carrier	Call B system for short. The carrier coordinate system is determined by the geographical coordinate system, and its state is represented by the attitude angle
Geography	Call G system for short.
Navigation	Call N system for short. The navigation coordinate system is the coordinate system using in strapdown inertial navigation system to solve the navigation parameters.

With the help of dynamic definition of Euler angles, these four coordinate systems can be transformed by Euler angles continuous rotation. It can be known from the definition of the above four coordinate systems, the attitude angle of carrier platform is determined by azimuth, apex angle and tool face angle, and these angles are Euler angles which are transformation angles between navigation coordinate system and carrier coordinate system (Titterton et al., 2004). Figure 2 shows Euler angles transformation between navigation coordinate system and carrier coordinate system.

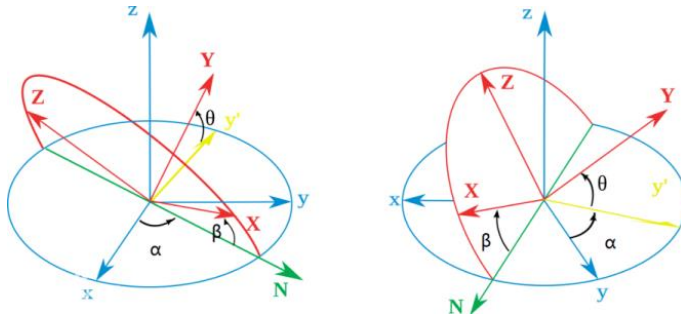


Figure 2: The Euler angles transformation

The transition matrix between navigation coordinate system and carrier coordinate system is shown in Eq(1).

$$C_n^b = \begin{bmatrix} \cos \alpha \cos \theta & \sin \alpha \cos \theta & -\sin \theta \\ \cos \alpha \sin \theta \sin \beta - \sin \alpha \cos \beta & \sin \alpha \sin \theta \sin \beta + \cos \alpha \cos \beta & \cos \theta \sin \beta \\ \cos \alpha \sin \theta \cos \beta + \sin \alpha \sin \beta & \sin \alpha \sin \theta \cos \beta - \cos \alpha \sin \beta & \cos \theta \cos \beta \end{bmatrix} \quad (1)$$

In Eq(1),  $\alpha$  is the angle of rotation around the rotating shaft, and  $\cos \beta_x$ ,  $\cos \beta_y$ ,  $\cos \beta_z$  are the components of the rotation axis in the X, y, and Z direction. The ordinary differential equations are solved by four order Runge Kutta Curta (R-K) method, azimuth  $\alpha$ , apex angle  $\theta$  and tool face angle  $\beta$  can be determined by Eq(2).

$$\begin{cases} \alpha = \arctan \left[ \frac{2(q_1 q_2 + q_0 q_3)}{q_0^2 + q_1^2 - q_2^2 - q_3^2} \right] \\ \theta = \arcsin \left[ 2(q_1 q_3 - q_0 q_2) \right] \\ \beta = \arctan \left[ \frac{2(q_2 q_3 + q_0 q_1)}{q_0^2 + q_1^2 - q_2^2 + q_3^2} \right] \end{cases} \quad (2)$$

## 2.2 Technical parameters

The SAR system developed and operated by Fraunhofer FHR, and it usually installed onboard a C-160 Transall airplane (Schimpf et al., 2010). The SAR system was complemented by a differential GPS (DGPS) system working at 20 Hz and a precise inertial measurement unit (IMU or inertial navigation system/INS) working at 500 Hz. A three-axis accelerometer was installed directly on the SAR antenna assembly. Additional detailed system characteristics, available baselines and corresponding ambiguity heights for a standard setup can be found in Table 3.

Table 3: Technical parameters and a standard setup configuration

Technical parameters	Value
Carrier frequencies	35 GHz(Ka-band), 94 GHz(W-band)
Bandwidth and PRF	900MHz, 1500 MHz(Stepped-frequency)
azimuth angle and apex angle	20-40° ±0.15° , 0-360° ±1.5°
Altitude	300-1000m
Receiving horns	R <sub>1</sub> , R <sub>2</sub> , B <sub>1</sub> =0.055
Ambiguity height(m)	208.41

## 3. Motion compensation-induced phase error correction

The analysis has been presented in two steps, mainly including raw data focusing and phase error correction with strapdown inertial navigation system. First the raw data focusing is reviewed briefly, followed by descriptions of additional calibrations of the antenna position and beam orientation. The interferometric chain is presented in the second step with its two variants using: 1) C2F phase unwrapping and 2) MAXIMUM LIKELIHOOD PHASE ESTIMATION phase estimation. The latter is described in more detail, including a constant phase offset removal required in a calibration step. Corrections for interferometric phase errors, including elevation-dependent phase errors and errors related to imperfect motion compensation are outlined. This paper focuses on motion compensation-induced phase error correction with strapdown inertial navigation system.

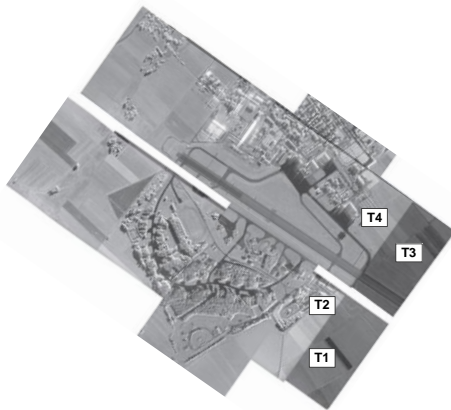


Figure 3: Overview of acquisitions T1–T4 at Xinpu in Qingdao

The phase-to-height conversion model uses an approximated baseline calculated as the position difference between the linearized tracks. This approximation would deliver exact results only given perfect motion compensation, if the height used for the motion compensation were accurate or if the true baseline vector matched the approximated baseline vector. The error introduced through the used phase-to-height model and the approximated baseline thus mainly depends on the difference between the real and “linearized” baseline vector combined with the difference between the real off-nadir angle and the value used in the motion compensation. This error was identified as a potential error source when using the interferometric height estimation method with the help of strapdown inertial navigation system. Figure 3 shows the geocoded amplitude images from all six acquisitions as a mosaic, and overview of acquisitions M1–M4 is at Xinpu in Qingdao, China.

To enhance the visibility of all acquisitions, two different radiometric scaling factors were employed for the geocoded amplitude images. Table 4 summarizes the geometrical characteristics of these acquisitions. The data of acquisitions overview characteristics are shown in table 4.

Table 4: The data of acquisitions overview characteristics in Qingdao Xinpu

Acquisitions	T1	T2	T3	T4
Acquisitions length(km)	2.2	2.36	2.33	2.15
Heading(°)	180	260	180	260
Illumination direction(°)	90	160	90	160
Mean sensor altitude	880m			
Near sensor altitude	1300m			
Range swath width	660m			

#### 4. Result analysis

The antenna tilt angle measurement, antenna beam pointing calibration (pitch and heading adjustment) and motion compensation-induced phase correction were crucial steps for improving the results presented in figure 4 and for allowing maximum likelihood phase estimation. These activities are shortly presented in the appendix, as they are not the main focus of this paper. The figure 4 shows that negative elevation angle values are below the beam center both ML and C2F method, while positive values are above the beam center.

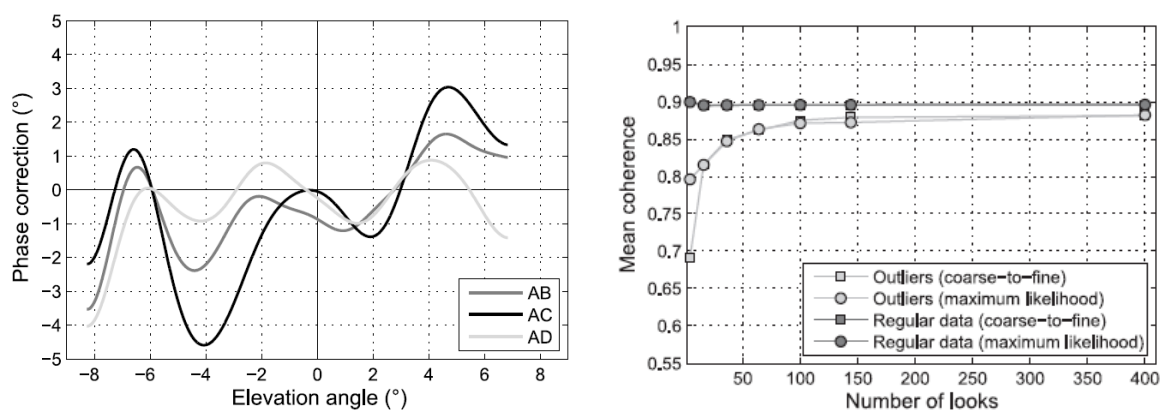


Figure 4: Coherence of regular data and outliers for both ML and C2F method

In the following, the effect of the elevation angle-dependent phase correction is shown. Then an example of the maximum likelihood phase estimation for a single point is given. Next, the results collected on a set of flat homogeneous surfaces with high coherence are analysed. We compare the measured noise level and the distribution of outliers between both maximum likelihood phase estimation and C2F methods. Finally, the statistical significance of the noise levels is tested, and the measurement accuracy can be guaranteed.

## 5. Conclusions

This paper puts forward a spaceborne SAR interferometry system operates on the strapdown inertial navigation mechanism, which is based on maximum likelihood phase estimation method. Then, in order to focus the NLFM airborne SAR data, a modified imaging RMA integrating a two steps has been proposed. Because a nonlinear frequency- modulation (NLFM) chirp waveform can shape the signal's power spectral density and provide a radar matched filter output with lower sidelobes without loss of the signal-to-noise ratio, in the method both the simulated and experimental imaging results validate the proposed generation of the NLFM waveform and the imaging algorithm.

Inertial navigation technology is completely independent of the measurement method, it does not depend on the external light, electromagnetic wave, sound, magnetic field and so on external information to measure the object angular motion and linear motion, so the working mode completely unaffected by the interference effects of the external environment. We compare the measured noise level and the distribution of outliers between both maximum likelihood phase estimation and C2F methods. Finally, the statistical significance of the noise levels is tested, and with the help of strapdown inertial navigation mechanism and compared to simulated data, dealing with real data implies that several calibration steps be carried out to ensure that the data fits the model, and the measurement accuracy can be guaranteed.

## Reference

- Feng F., Ai C., Xu H., Cui Z., Gao C., 2015, Research on the condition model of drilling fluid non-retention in eccentric annulus, *International Journal of Heat and Technology*, 33(1):9-16. Doi: 10.18280/ijht.330102
- Magnard C., Frioud M., Small D., Brehm T., 2015, Analysis of a Maximum Likelihood Phase Estimation Method for Spaceborne Multibaseline SAR Interferometry, *IEEE Journal of Selected Topics in Applied Earth Observations & Remote Sensing*, 22(4): 1-14.
- Perez R., Costa U., Torrent M., Solana J., 2010, Upper limb portable motion analysis system based on inertial technology for neurorehabilitation purposes, *sensors*, 10(12): 10733-10751.
- Reigber A., Alivizatos E., Potsis A., Moreira A., 2006, Extended wavenumber-domain synthetic aperture radar focusing with integrated motion compensation, *IEE Proc. Radar Sonar Navigation.*, 153(3): 301–310. Doi: 10.1049/ip-rsn:20045087
- Schimpf H., Essen H., Boehmsdorff S., Brehm T., 2002, MEMPHIS — A fully polarimetric experimental radar, in *Proc. IEEE Int. Geosci. Remote Sens. Symp. (IGARSS)*. 2002(3). 1714–1716.
- Schmitt M., Stilla, U., 2014, Maximum-likelihood-based approach for single-pass synthetic aperture radar tomography over urban areas, *IET Radar Sonar Navigation.*, 8(9):1145–1153. Doi: 10.1049/iet-rsn.2013.0378
- Singh S.N., Singh D.K., 2015, Study of combined free convection and surface radiation in closed cavities partially heated from below, *International journal of heat and technology*, 33(2):1-8. Doi: 10.18280/ijht.330201
- Titterton D., Weston J., 2004, Strapdown inertial navigation technology. *Institution of Electrical Engineers*, 20(7): 33 - 34.
- Vizitiu I., Anton L., Popescu F., Iubu G., 2012, The synthesis of some NLFM laws using the stationary phase principle, in *Proc. IEEE ISETC, Timisoara, U.K.*, 2012:377–380.
- Yang L., Bi G., Xing M., Zhang L., 2015, Spaceborne SAR Moving Target Signatures and Imagery Based on LVD, *IEEE Transactions on Geoscience & Remote Sensing*, 53(11): 5958-5971.